Oral exposure to polyethylene microplastics induces inflammatory and metabolic changes and promotes fibrosis in mouse liver.

Madjid Djouina, Christophe Waxin, Laurent Dubuquoy, David Launay, Cecile Vignal, Mathilde Body-Malapel

Ecotoxicology and Environmental Safety 264 (2023) 115417

Contents lists available at ScienceDirect

Ecotoxicology and Environmental Safety

journal homepage: www.elsevier.com/locate/ecoenv

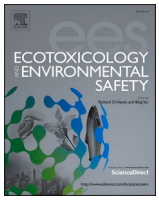

Oral exposure to polyethylene microplastics induces inflammatory and metabolic changes and promotes fibrosis in mouse liver.

Madjid Djouina, Christophe Waxin, Laurent Dubuquoy, David Launay, Cécile Vignal, Mathilde Body-Malapel *

Univ. Lille, Inserm, CHU Lille, U1286- INFINITE - Institute for Translational Research in Inflammation, F-59000 Lille, France

A R T I C L E I N F O

Keywords:
Microplastics
Polyethylene
Mice
Liver
Fibrosis
Lipid metabolism

A B S T R A C T

Accumulating evidence shows widespread contamination of water sources and food with microplastics. Although the liver is one of the main sites of bioaccumulation within the human body, it is still unclear whether microplastics produce damaging effects. In particular, the hepatic consequences of ingesting polyethylene (PE) microplastics in mammals are unknown. In this study, female mice were fed with food contaminated with 36 and 116 μm diameter PE microbeads at a dosage of 100 μg/g of food for 6 and 9 weeks. Mice were exposed to each type of microbead, or co-exposed to the 2 types of microbeads. Mouse liver showed altered levels of genes involved in uptake, synthesis, and β-oxidation of fatty acids. Ingestion of PE microbeads disturbed the detoxification response, promoted oxidative imbalance, increased inflammatory foci and cytokine expression, and enhanced proliferation in liver. Since relative expression of the hepatic stellate cell marker *Pdgfa* and collagen deposition were increased following PE exposure, we assessed the effect of PE ingestion in a mouse model of CCl_4-induced fibrosis and showed that PE dietary exposure exacerbated liver fibrogenesis. These findings provide the first demonstration of the adverse hepatic effects of PE ingestion in mammals and highlight the need for further health risk assessment in humans.

1. Introduction

In the wake of industrial development and anthropogenic activities, a dramatic expansion in global production chains for plastic goods has occurred over the past several decades (Lim, 2021). Currently, about 400 million tons of plastic materials are produced each year, and this is projected to double by 2050 (Lim, 2021). Due to accelerated production and limited reuse, transformation, and recycling initiatives, the world's ability to handle the excess of used plastic products has been overwhelmed (Ferronato and Torretta, 2019). Once discarded in nature, plastic waste is exposed to physical (e.g., ultraviolet radiation and temperature), chemical (e.g., salinity, pH, and corrosive agents), and biological (e.g., bacteria, microalgae, and plankton) factors that cleave these materials into microplastic (MP; 1–5000 μm in diameter) and nanoplastic (NP; <1 μm) particles (Hirt and Body-Malapel, 2020; Song et al., 2017).

Humans are exposed to MPs every day. They are omnipresent in our food, beverages, water, and air (Gasperi et al., 2018; Mortensen et al., 2021). A recent study estimated MP median intake rates are 553 and 883 particles/capita/day for children and adults, respectively. This intake can lead to irreversible accumulation in tissues of 8.32×10^3 particles/capita for children and up to 5.01×10^4 particles/capita for adults (Mohamed Nor et al., 2021). Human exposure to MPs starts *in utero* and lasts a lifetime. For example, a pilot study detected MPs in meconium sampled during two cesarean sections for breech deliveries (Braun et al., 2021). Another study that analyzed MPs in three meconium as well as 6 infant and 10 adult fecal samples concluded that MP concentrations were significantly higher in infant than in adult stool (J. Zhang et al., 2021a). Several studies have detected various MPs in human adult stool (Luqman et al., 2021; Schwabl et al., 2019; Wibowo et al., 2021). MPs were also found in human colectomy and cirrhotic samples (Horvatits et al., 2022; Ibrahim et al., 2021). Furthermore, accumulating evidence from human and mouse studies have shown that MPs disrupt the integrity of the intestinal barrier, enter the bloodstream (Leslie et al., 2022; Sun et al., 2022), and accumulate in different tissues and organs such as gut, liver, brain, and kidney (Deng et al., 2017; Im et al., 2022;

* Correspondence to: Institute for Translational Research in Inflammation, INFINITE - Univ. Lille, Inserm, CHU Lille, U1286, Faculté de Médecine - Pôle Recherche, 4éme étage Centre, Place Verdun, F-59045 Lille, France.
E-mail address: mathilde.body@univ-lille.fr (M. Body-Malapel).

https://doi.org/10.1016/j.ecoenv.2023.115417
Received 20 June 2023; Received in revised form 23 August 2023; Accepted 26 August 2023
Available online 29 August 2023

Mu et al., 2022).

As the main bioaccumulation target of MPs, the liver has been the subject of several studies on the impact of MP ingestion in mice. Hepatotoxicity and lipid metabolism disturbances have been observed after ingestion of polystyrene (PS) MPs (Cheng et al., 2022a; Lu et al., 2018). Oral exposure to PS MPs induced oxidative stress (Deng et al., 2017; Mu et al., 2022) and promoted inflammation under basal and pathological conditions (Deng et al., 2017; Huang et al., 2022; Luo et al., 2022; Wen et al., 2022; Zhao et al., 2021; Zheng et al., 2021). Several hallmarks of hepatotoxicity were also observed following chronic exposure to polyvinyl chloride (PVC) MPs (Chen et al., 2022).

Although PE is the most abundant polymer in raw and treated drinking water and bottled mineral water (Mortensen et al., 2021), and one of the most common monomers found in human food (Bai et al., 2022), little is known regarding its effect on mammalian liver. Thus far it has been reported that PE MP exposure induces liver damage in several aquatic organisms (da Costa Araújo et al., 2020; Dong et al., 2022; Hu et al., 2022; Lu et al., 2022; Mak et al., 2019). Therefore, the purpose of this study was to explore the hepatic effects of sub-chronic PE MP exposure in mice.

2. Methods and materials

2.1. Particles

PE microbeads were acquired from Cospheric (Santa Barbara, USA). Two categories of microbeads were used: red fluorescent beads (RB; item# UVPMS-BR-1.090; 10–45 μm) and green fluorescent beads (GB; item# UVPMS-BG-1.00; 106–125 μm). Size range and polymeric composition were characterized in a previous study (Djouina et al., 2022a). The median size of microbeads was 36 and 116 μm for RB and GB, respectively. Both were composed of a pure PE polymer as confirmed by Fourier transform infrared spectra.

2.2. Mice and experimental protocols

All animal procedures were conducted in accordance with institutional guidelines approved by the Animal Care and Ethical Use Committee of the University of Lille (committee no.75; authorization no. APAFIS #38663–2022082613292602). C57BL/6 mice were purchased from Janvier Labs (Le Genest-Saint-Isle, France) and housed under standard conditions. Female mice from 7 to 12 weeks old were used in the study.

In the first set of experiments, mice were randomly assigned to 4 experimental groups (n = 10/group): 1) control group, receiving control food; 2) RB group, receiving food spiked with 100 μg RB microbeads/g of food; 3) GB group, receiving food spiked with 100 μg of GB microbeads/g of food; and 4) RB+GB group, receiving food spiked with 100 μg each of RB and GB microbeads/g of food. The concentration of PE microbeads added to food was 100 μg/g since this amount is within the realistic range of human ingestion levels (Djouina et al., 2022a; Senathirajah et al., 2021). Treatment periods were either 6 or 9 weeks. Blood and liver were sampled at necropsy.

In the second set of experiments, to induce chronic liver fibrosis, 8-week old C57BL/6 female mice were injected with CCl_4 (Sigma-Aldrich; 0.2 ml/kg; in olive oil at a ratio of 1:4; *i.p.* injection twice a week for 8 weeks). Mice were randomly divided into 5 groups (n = 8/group): 1) control group, receiving control food and olive oil *i.p.* repeated injections; 2) CCl_4 group, receiving control food and CCl_4 repeated injections; 3) CCl_4 +RB group, receiving food spiked with 100 μg of RB microbeads/g of food and CCl_4 repeated injections; 4) CCl_4 +GB group, receiving food spiked with 100 μg of GB microbeads/g of food and CCl_4 repeated injections; and 5) CCl_4 +RB+GB group, receiving food spiked with 100 μg each of RB and GB microbeads/g of food and CCl_4 repeated injections. Animals were sacrificed 24 h after the last injection of CCl_4. Blood and liver were sampled at necropsy.

2.3. Serum enzyme activity

Serum activity of alanine transaminase (ALT) and aspartate aminotransferase (AST) were measured using commercial kits (MAK052 and MAK055, Sigma-Aldrich). The optical density (OD) at 570 nm for ALT and 450 nm for AST was measured using a microplate reader (FluostarOmega, BMG Labtech). Following incubation for 2–3 min at 37 °C, initial absorbance was recorded and kinetic measurements were recorded every 5 min for 1 h. Pyruvate and glutamate were used as standards for ALT and AST, respectively. ΔOD was calculated and ALT and AST activities were derived based on the ratio of ΔOD and reaction time.

2.4. Liver total cholesterol, triglyceride, and free fatty acid content measurements

To isolate lipids, liver samples (~50 mg) were homogenized in 1 ml of 2:1 (v/v) chloroform-methanol mixture. Following centrifugation at 1000 g, 1 ml of supernatant was recovered and 200 μl of distilled water was added. Samples were centrifuged at 650 g and the organic layer was removed, evaporated for 24 h, and reconstituted in isopropanol. Triglyceride content was measured with Triglyceride Reagent (T2449, Sigma-Aldrich) and Free Glycerol Reagent (T2449, Sigma-Aldrich). Glycerol Standard (G7793, Sigma-Aldrich) was used as a reference standard. OD was measured at 450 nm. Total cholesterol and free fatty acids were assayed using commercially available kits (Cholesterol FS # 1 1300 99 10 021, DiaSys, and free fatty acid quantification kit, MAK044, Sigma-Aldrich, respectively).

2.5. Liver histological analysis

Liver was fixed in 4% formaldehyde overnight, processed, and embedded in paraffin wax by an automatic sample preparation system (LOGOS One, Milestone). Serial histological sections of 4 μm thickness were cut, deparaffinized, rehydrated for hematoxylin and eosin (H&E) staining (05–06004/L, 05–10007/L, Bio-Optica) or sirius red staining (P6744 and 365548, Sigma-Aldrich). The slides were scanned on a Zeiss AxioScan.Z1® slide scanner (Zeiss, Jena, Germany) at 20X magnification.

Whole tissue was analyzed with QuPath software (version 0.4.1.) (Bankhead et al., 2017). To localize and quantify inflammatory foci, the "Cell Detection" command was used followed by the "Cell Classification" command for identification of immune cells. Each inflammatory focus was manually drawn, measured, and counted. To quantify sirius red staining, the “Estimate Stain Vectors” command was applied to each slide and then the percentage of staining was calculated with the “Positive Cell Detection” command.

2.6. Immunohistochemical staining and quantification

Serial histological sections of 4 μm thickness were cut, deparaffinized, and rehydrated. For antigen unmasking, sections were placed in 10 mM sodium citrate buffer (pH 6.0) and incubated in a heat-induced antigen retrieval chamber for 20 min at 121 °C. After washing, sections were blocked for 30 min with 5% goat serum. Rabbit anti-mouse Ki-67 primary antibody (MA5–14520, Invitrogen) and rabbit anti-mouse alpha-smooth muscle actin (α-SMA) primary antibody (#19245, Signaling Technology) were then incubated overnight at 4 °C (1:200 dilution). After washing, tissue sections were incubated for 30 min at room temperature with ImmPRESS® HRP Goat Anti-Rabbit IgG Polymer Detection Kit (Vector Laboratories, Inc., United States) and staining was exposed with SignalStain® DAB Substrate (#8059, Cell Signaling Technology). Nuclear staining with hematoxylin was performed before addition of mounting medium. The slides were then scanned under 20X magnification as described earlier. Immunostaining quantification was performed with QuPath software. The percentage of cells positive for either Ki-67 or α-SMA staining was calculated with the

"Positive Cell Detection" command.

For apoptosis analysis in liver sections, the In Situ Cell Death Detection Kit, TMR red TUNEL technology (#12156792910, Roche) was performed according to manufacturer's specifications. Tissue sections were dewaxed, rehydrated as described earlier, and pretreated in permeabilization solution (0.1% Triton X-100 *, 0.1% sodium citrate) for 8 min. After washing, the samples were labeled with the TUNEL reaction mixture and incubated for 60 min at + 37 °C in a humidified atmosphere in the dark. Sections were counterstained with DAPI (Molecular Probes, Eugene OR, USA). The slides were then scanned at 20X magnification and the percentage of positive cells was quantified with the "Positive Cell Detection" command in QuPath software.

2.7. Real-time quantitative polymerase chain reaction (RT-qPCR)

Liver tissue samples were homogenized with ceramic beads using a FastPrep-24 tissue homogenizer (MP Biomedical). Total RNA was extracted with the NucleoSpin® RNA kit (Macherey-Nagel). Transcript levels of genes were quantified with the StepOne™ Real-Time PCR system using a SYBR Green PCR master mix (Thermo Fisher Scientific). The primer sequences were designed using Primer Express 3 (Thermo Fisher Scientific) and are available upon request. Melting curve analyses were performed for each sample and gene to confirm the specificity of the amplification. The relative expression of each target gene was normalized to the relative expression of the *Polr2a* gene. Quantification of target gene expression was based on the comparative cycle threshold (Ct) value. The fold changes in the target genes were analyzed by the $2^{-\Delta\Delta Ct}$ method.

2.8. Liver malondialdehyde (MDA) analysis

Liver lysates were incubated with acetic acid and sodium dodecyl sulfate at 95 °C for 1 h, followed by centrifugation at 800 g for 10 min. Supernatants were transferred to a black 96-well plate and the fluorescence intensity was measured at $\lambda_{ex} = 532$ and $\lambda_{em} = 553$ nm. 1,1,3,3-Tetramethoxypropane (Sigma-Aldrich) was used as a standard. Protein concentration in samples was determined using the DC™ protein assay (Bio-Rad Laboratories). Liver MDA concentration was normalized by the sample protein concentration and expressed as nanomoles per mg of protein.

2.9. Statistics

Results are expressed as mean ± standard error of the mean. The statistical significance of differences between experimental groups was calculated using the Mann-Whitney nonparametric U test (GraphPad Prism software, USA). Statistical significance was defined as $p < 0.05$.

3. Results

Exposure to 36 μm RB and 116 μm GB PE microbeads individually or in combination for 6 and 9 weeks did not induce mouse mortality, gross clinical symptoms, or significant body weight variation compared to the control group (Suppl. Fig. 1A). After 9 weeks of exposure, the mice exposed to RB-contaminated diet showed increased serum AST and ALT activities, suggesting potential hepatotoxicity of PE microbeads (Suppl. Fig. 1B).

3.1. PE microbeads cause disturbances in liver lipid metabolism

Hepatic transcriptional levels of genes related to fatty acid metabolism were evaluated using RT-qPCR to determine the effect of PE microbead exposure (Luo et al., 2019; X. Wang et al., 2023b). After a 6-week administration period, the relative expression of two genes

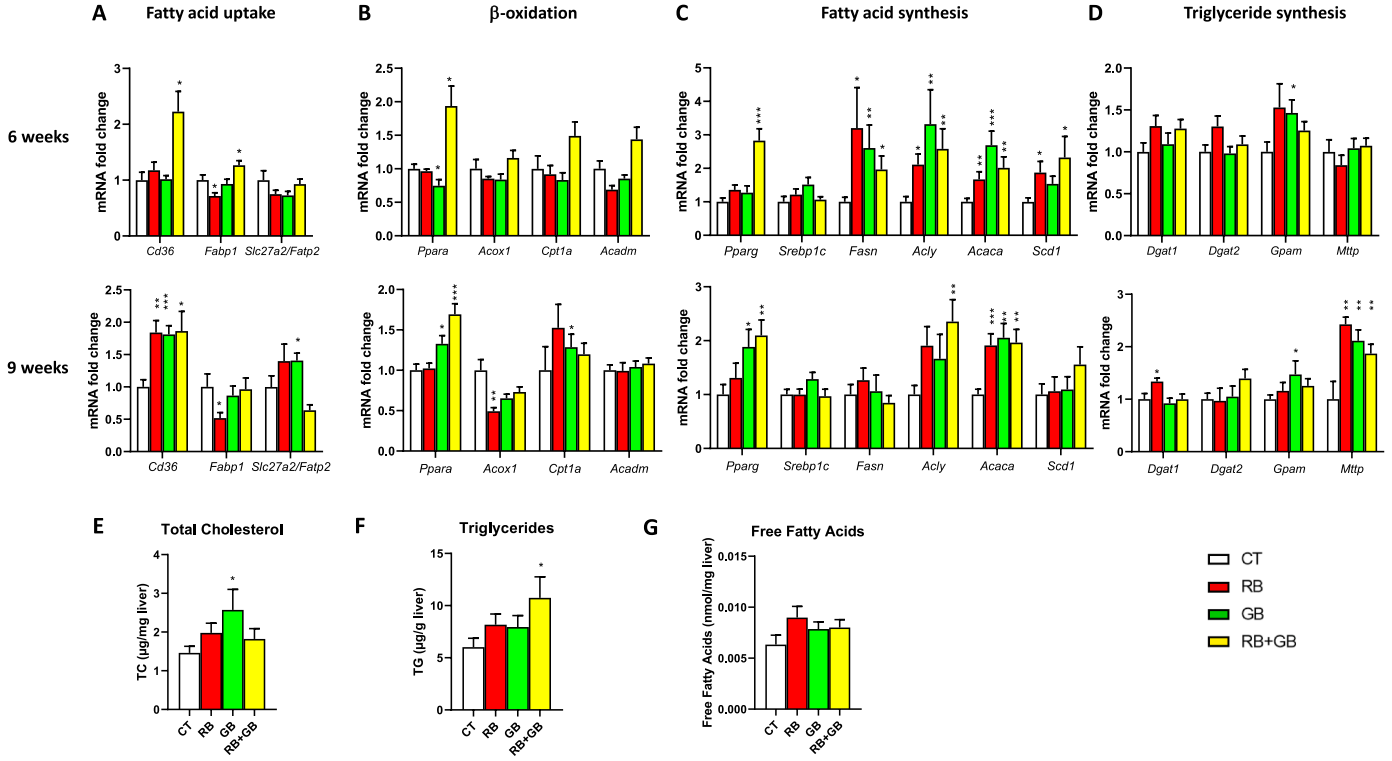

Fig. 1. Effects of polyethylene (PE) exposure on liver lipid metabolism. Mice were exposed to food spiked with 100 μg/g of PE microbeads (red beads (RB), green beads (GB), or RB+GB; n = 10/group) or control food (CT; n = 10) for 6 and 9 weeks. Gene expression was quantified by RT-qPCR for (A) fatty acid uptake markers, (B) β-oxidation markers, (C) fatty acid synthesis markers, and (D) triglyceride synthesis markers. In addition, biochemical analysis of liver (E) cholesterol, (F) triglyceride and (G) free fatty acid levels were assessed. Upper panel: 6 weeks exposure. Medium and lower panel: 9 weeks exposure. * $p < 0.05$, * * $p < 0.01$, * ** $p < 0.005$, and * ** * $p < 0.001$ compared to the control group as determined by the Mann-Whitney U test.

involved in fatty acid uptake, platelet glycoprotein 4 (*Cd36*) and fatty acid binding-protein, liver (*Fabp1*), were increased in mice exposed to RB+GB contaminated food as compared to control mice (Fig. 1A). Exposure to RB-contaminated food induced downregulation of *Fabp1* in liver. The third marker of fatty uptake, long-chain fatty acid transport protein 2 *Slc27a2/Fatp2*, was not modified by PE dietary exposure. A two-fold increase in expression of the peroxisome proliferator-activated receptor alpha (*Ppara*) gene was detected after exposure to both types of PE microbeads, whereas the transcription of the others genes involved in β-oxidation, including peroxisomal acyl-coenzyme A oxidase 1 (*Acox1*), carnitine O-palmitoyltransferase 1, liver isoform (*Cpt1a*), and medium-chain specific acyl-CoA dehydrogenase, mitochondrial (*Acadm*), did not vary between groups (Fig. 1B). For genes involved in fatty acid synthesis, levels of peroxisome proliferator-activated receptor gamma (*Pparg*) and acyl-CoA desaturase 1 (*Scd1*) were elevated in the liver of RB+GB exposed mice, and fatty acid synthase (*Fasn*), ATP-citrate lyase (*Acly*), and acetyl-CoA carboxylase 1 (*Acaca*) were significantly upregulated in all groups of PE-exposed mice (Fig. 1C). Genes involved in triglyceride synthesis, diacylglycerol O-acyltransferase 1 (*Dgat1*), diacylglycerol O-acyltransferase 2 (*Dgat2*), glycerol-3-phosphate acyltransferase 1, mitochondrial (*Gpam*), and microsomal triglyceride transfer protein large subunit (*Mttp*), were not modified by PE exposure, with the exception of *Gpam* which was increased in GB-exposed mice (Fig. 1D). After 9-week exposure, significant modulation of fatty acid metabolism markers was also observed. Exposure to RB microbeads downregulated the expression of *Fabp1* and *Acox1* and upregulated the expression of *Dgat1*. Exposure to GB microbeads increased the levels of *Fatp2*, *Cpt1a*, and *Gpam*. Expression of *Ppara* and *Pparg* was higher in liver of mice exposed to GB and RB+GB. The relative expression of *Cd36*, *Acaca*, and *Mttp* was increased in all groups of PE-exposed mice. In summary, dietary exposure to PE microbeads disturbed genes associated with fatty acid metabolism in favor of increased mRNA levels of genes associated with fatty acid uptake, *β*-oxidation, and synthesis.

Biochemical parameters of the liver were also evaluated. Liver cholesterol levels were significantly increased in mice fed with food contaminated with GB microbeads (Fig. 1E). Hepatic triglycerides were elevated in mice exposed to RB+GB-contaminated food (Fig. 1F). The hepatic levels of free fatty acids were not significantly modified (Fig. 1G). Taken together, these data show that dietary exposure to PE microbeads altered lipid metabolism in liver of exposed mice.

3.2. PE microbeads alter liver detoxification and oxidative defense biomarkers

Hepatic metabolism is generally conducted in two phases and carried out by distinct groups of enzymes. For phase 1, hepatic cytochrome p450 (Cyp) is the main enzyme group. Among this gene family, *Cyp2a4* and *Cyp2b10* mRNA levels were increased in the three groups of PE-exposed mice after 6-week exposure (Fig. 2A). The upregulation of *Cyp2a4* in liver was also observed after 9-week exposure. The main phase 2 xenobiotic metabolizing enzymes are glutathione S-transferases and UDP glucuronosyl-transferases. Levels of *Gsta1* were upregulated in livers of mice exposed to RB, GB, and RB+GB after 6 weeks, and *Ugt1a1* in liver of RB+GB-exposed mice after 9-week exposure.

The effect of PE dietary exposure was evaluated using biomarkers of liver oxidative stress. In 6-week exposed mice, transcripts of nitric oxide synthase, inducible (*Nos2*), catalase (*Cat*), nuclear factor erythroid 2-related 2 (*Nfe2l2*), NAD(P)H dehydrogenase [quinone] 1 (*Nqo1*), and heme oxygenase 1 (*Hmox1*) were elevated in mice fed RB+GB (Fig. 2B) and *Cat* levels were decreased in liver of mice fed RB-contaminated food. Superoxide dismutase [Cu-Zn] (*Sod1*), superoxide dismutase [Mn], mitochondrial (*Sod2*), and glutathione peroxidase 1 (*Gpx1*) relative levels were not modified. In 9-week exposed mice, *Nfe2l2* was upregulated in GB-exposed mice and *Nqo1* was overexpressed in mice exposed to RB and RB+GB. *Hmox1* transcription was increased in liver of mice fed RB, GB, and RB+GB. Liver MDA content, a marker of lipid peroxidation levels, was decreased in mice exposed to RB for 6 weeks, and increased in mice exposed to RB+GB for 6 weeks and to RB for 9 weeks (Fig. 2C). Therefore, in mice, the processes of detoxification and oxidative defense were altered by dietary exposure to PE microbeads.

3.3. Effect of PE microbeads on liver inflammation

H&E staining was used to analyze histological changes within liver tissues (Fig. 3A). No overt signs of necrosis, ballooning, edema, or hyperemia were observed. As focal inflammation is the most frequently observed inflammatory lesion of liver in rodent toxicity studies, the number and size of the inflammatory foci present in hepatic parenchyma were quantified (Oliveira et al., 2019) (Fig. 3A-B). Although the abundance of inflammatory foci was unmodified, their size was significantly increased in liver of mice exposed to RB+GB for 6 weeks compared to controls. After 9-week exposure, the inflammatory foci were more numerous in mice exposed to GB and RB+GB. There was a similar trend for the size of inflammatory foci with a significance threshold reached

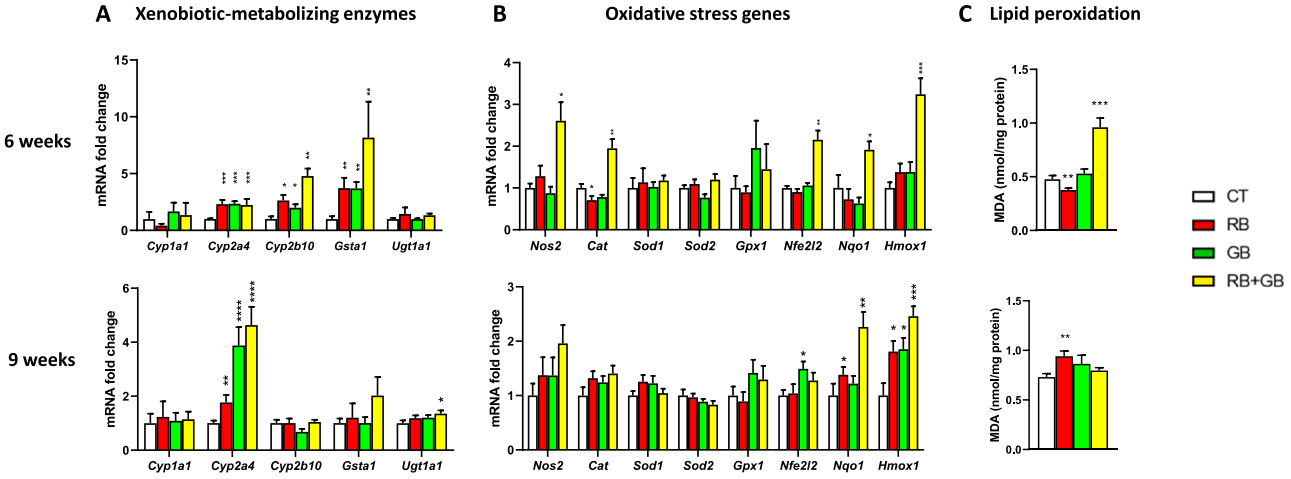

Fig. 2. Effects of polyethylene (PE) exposure on liver xenobiotic metabolism and oxidative stress markers. Mice were exposed to food spiked with 100 μg/g of PE microbeads (red beads (RB), green beads (GB), or RB+GB; n = 10/group) or control food (CT; n = 10) for 6 and 9 weeks. Gene expression was quantified by RT-qPCR for (A) xenobiotic-metabolizing enzymes, and (B) oxidative stress genes. (C) Analysis of liver MDA levels. Upper panel: 6 weeks exposure. Lower panel: 9 weeks exposure. * $p < 0.05$, * * $p < 0.01$, * ** $p < 0.005$, and * ** * $p < 0.001$ compared to the control group as determined by the Mann-Whitney U test.

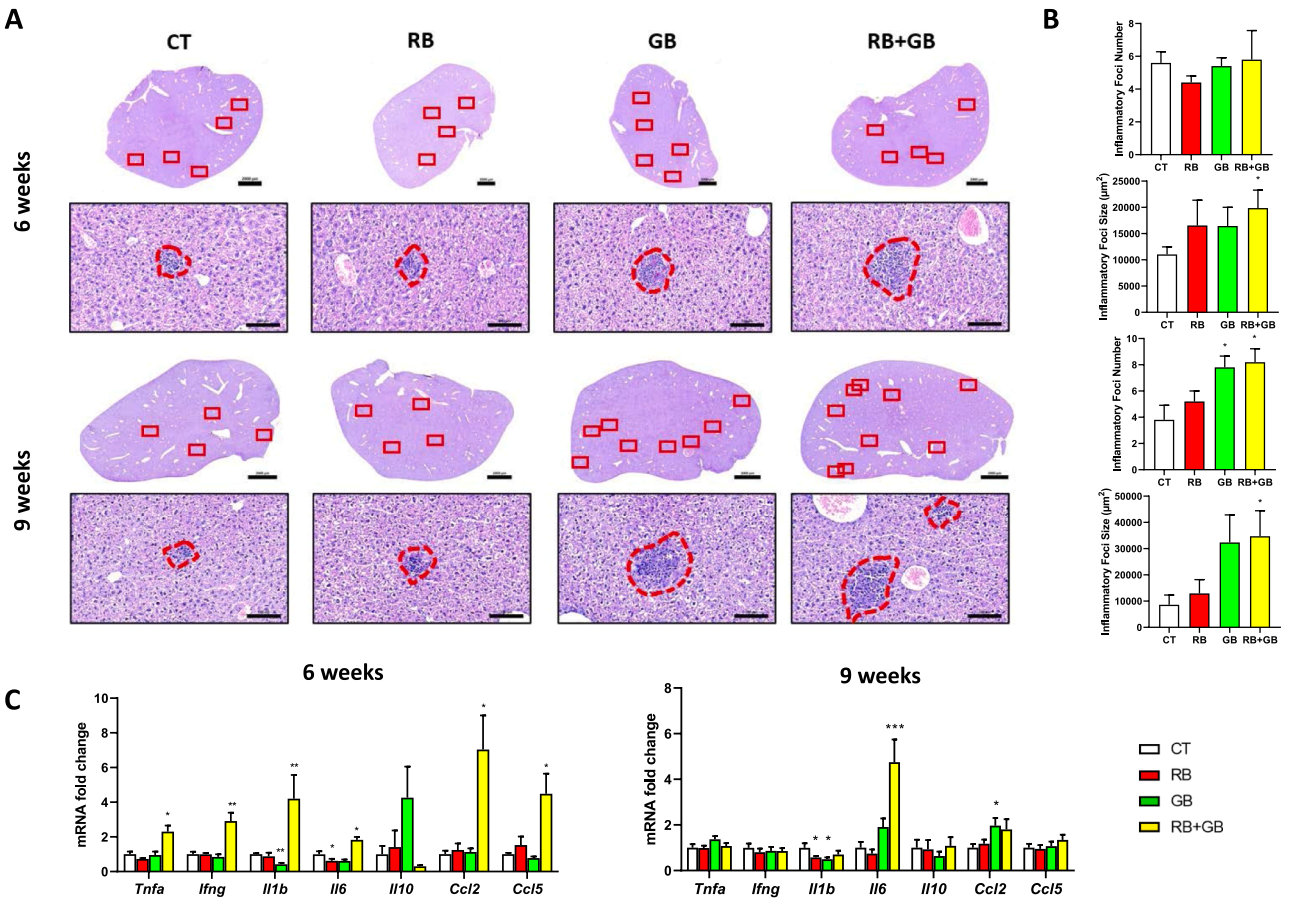

Fig. 3. Effects of polyethylene (PE) exposure on liver injury. Mice were exposed to food spiked with 100 µg/g of PE microbeads (red beads (RB), green beads (GB), or RB+GB; n = 10/group) or control food (CT; n = 10) for 6 and 9 weeks. (A-B) Upper panel: 6 weeks exposure. Lower panel: 9 weeks exposure. (A) Representative pictures of liver sections stained with H&E. (B) Quantitative assessment of the number and size of inflammatory foci. (C) Gene expression of liver cytokines/chemokines. Left: 6 weeks exposure. Right: 9 weeks exposure. * $p < 0.05$, * * $p < 0.01$, * ** $p < 0.005$, and * ** * $p < 0.001$ compared to the control group as determined by the Mann-Whitney U test.

for the RB+GB group. Major liver cytokines and chemokines were quantified at the transcriptional level (Fig. 3C). After 6-week exposure, the mRNA abundance of tumor necrosis factor (*Tnf*), interferon gamma (*Ifng*), interleukin-1 beta (*Il1b*), interleukin-6 (*Il6*), CC motif chemokine 2 (*Ccl2*), and C-C motif chemokine 5 (*Ccl5*) were increased in mice fed RB+GB compared to control mice. Decreased levels of *Il1b* and *Il6* transcripts were also quantified in GB- and RB-exposed mice, respectively. After 9-week exposure, downregulation of *Il1b* was observed in both RB- and GB-exposed mice. *Il6* levels were highly elevated in liver of mice fed RB+GB. *CCl2* mRNA was upregulated in GB-exposed mice. These results show that co-exposure to RB and GB PE microbeads induced low grade inflammation of the liver.

3.4. PE microbeads induce liver cell proliferation

Proliferation marker protein Ki-67 (*Mki67*) is a marker of cell division and its overexpression is an indicator of proliferation (Dubuquoy et al., 2015). Relative mRNA expression of *Mki67* was increased after 6-week exposure to RB+GB, and after 9-week exposure to GB and RB+GB (Fig. 4A). Immunohistochemical staining of Ki-67 protein confirmed the increased number of Ki-67-positive cells in liver of mice exposed to RB+GB, both after 6- and 9-week exposure (Fig. 4B), showing that dietary exposure to PE increased cell proliferation in liver. Because apoptosis can be induced to protect the liver from an overshooting proliferative response (Campana et al., 2021), and PS MP exposure has been shown to induce liver apoptosis (Li et al., 2021; S. Wang et al., 2023a), we sought to determine whether apoptosis was affected in our experimental conditions (Fig. 4C). The TUNEL staining showed no modification of apoptosis by PE MP ingestion.

3.5. PE microbeads alter expression of hepatic cell markers

Markers of the main cell types in liver were quantified by RT-qPCR (Saleh et al., 2021; Yang et al., 2021). The levels of specific gene markers of hepatocytes, albumin (*Alb*) and hepatocyte nuclear factor 4-alpha (*Hnf4a*), were not modified after 6-week exposure but increased after 9-week exposure to RB+GB (Fig. 5A). The specific markers of cholangiocytes, hepatocyte nuclear factor 1-beta (*Hnf1b*) and transcription factor SOX-9 (*Sox9*), were increased in RB-exposed mice and decreased in GB-exposed mice after 6-week exposure (Fig. 5B). After 9-week exposure, *Hnf1b* mRNA was downregulated in GB-exposed mice and both *Hnf1b* and *Sox9* were decreased in mice fed RB+GB. The specific markers of hepatic stellate cells (HSCs), actin, aortic smooth muscle (*Acta2*) and platelet-derived growth factor subunit A (*Pdgfa*), were upregulated after 6-week exposure to RB+GB (Fig. 5C). After 9-week exposure, levels of *Pdgfa* were elevated in mice fed RB, GB, and RB+GB. The specific markers of portal fibroblasts, elastin (*Eln*) and Thy-1 membrane glycoprotein (*Thy1*), were unmodulated by dietary exposure to PE microbeads (Fig. 5D). The levels of the specific markers of Kupffer cells, macrosialin (*Cd68*) and C-type lectin domain family 4 member F (*Clec4f*), were unaltered after 6-week exposure but either downregulated (*Cd68*) or upregulated (*Clec4f*) after 9-week exposure to GB microbeads.

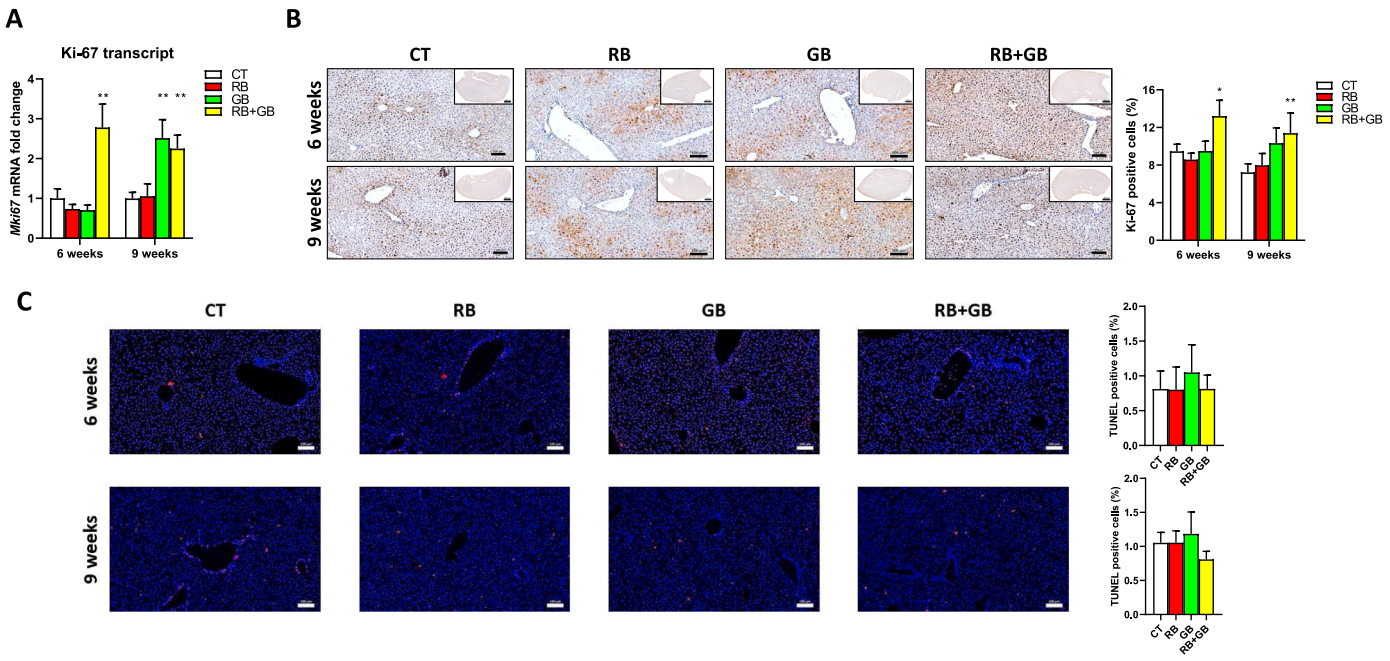

Fig. 4. Effects of polyethylene (PE) exposure on liver cell proliferation and apoptosis. Mice were exposed to food spiked with 100 μg/g of PE microbeads (red beads (RB), green beads (GB), or RB+GB; n = 10/group) or control food (CT; n = 10) for 6 and 9 weeks. (A) mRNA quantification of the proliferative marker Ki-67. (B) Representative pictures of Ki-67-stained liver and Ki-67 immunostaining quantification. (C) Representative pictures of TUNEL-stained liver and TUNEL immunostaining quantification * $p < 0.05$, * * $p < 0.01$, * ** $p < 0.005$, and * ** * $p < 0.001$ compared to the control group as determined by the Mann-Whitney U test.

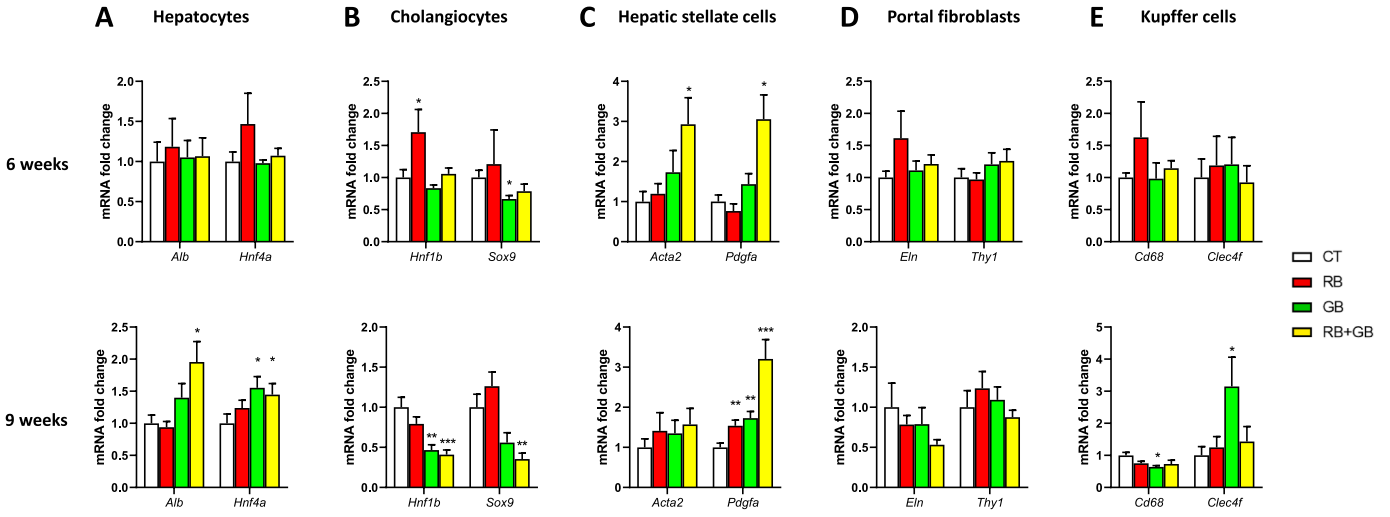

Fig. 5. Effects of polyethylene (PE) exposure on markers of main liver cell types. Mice were exposed to food spiked with 100 μg/g of PE microbeads (red beads (RB), green beads (GB), or RB+GB; n = 10/group) or control food (CT; n = 10) for 6 and 9 weeks. Gene quantification of cell type-specific biomarkers for (A) hepatocytes, (B) cholangiocytes, (C) hepatic stellate cells, (D) portal fibroblasts, and (E) Kupffer cells. Upper panel: 6 weeks exposure. Lower panel: 9 weeks exposure. * $p < 0.05$, * * $p < 0.01$, * ** $p < 0.005$, and * ** * $p < 0.001$ compared to the control group as determined by the Mann-Whitney U test.

3.6. PE microbeads exacerbate the development of CCl_4-induced liver fibrosis

Since at least one HSC marker was upregulated after both 6 and 9 weeks of combined PE MP exposure, we performed sirius red staining to assess collagen deposition and therefore HSC activation (Fig. 6). Sirius red positive areas were increased in liver of mice exposed to GB for 6 weeks (Fig. 6A) and exposed to GB and RB+GB for 9 weeks (Fig. 6B). Since the activation of HSCs and their conversion into myofibroblasts play key roles in the development of liver fibrosis, we assessed the effects of dietary exposure to PE microbeads in a mouse model of induced liver fibrosis by repeated *i.p.* administration of CCl_4. All CCl_4-induced groups showed a significant increase of serum AST and ALT activity levels compared to the control group (Fig. 7A). The elevated AST and ALT activity levels were significantly worsened in mice fed RB+GB compared to control mice. Sirius red staining and immunohistochemical staining of α-SMA were used to evaluate the degree of fibrosis (Fig. 7B). Results showed that collagen deposition and α-SMA protein were present in liver of mice repeatedly administered CCl_4, confirming the induction of hepatic fibrosis. This was also confirmed by the quantitative increase of both sirius red and α-SMA positive areas in all the CCl_4 fibrotic groups compared with the control group (Fig. 7C-D). Furthermore, the areas positive for sirius red and α-SMA were significantly increased in mice exposed to GB and RB+GB compared to fibrotic mice

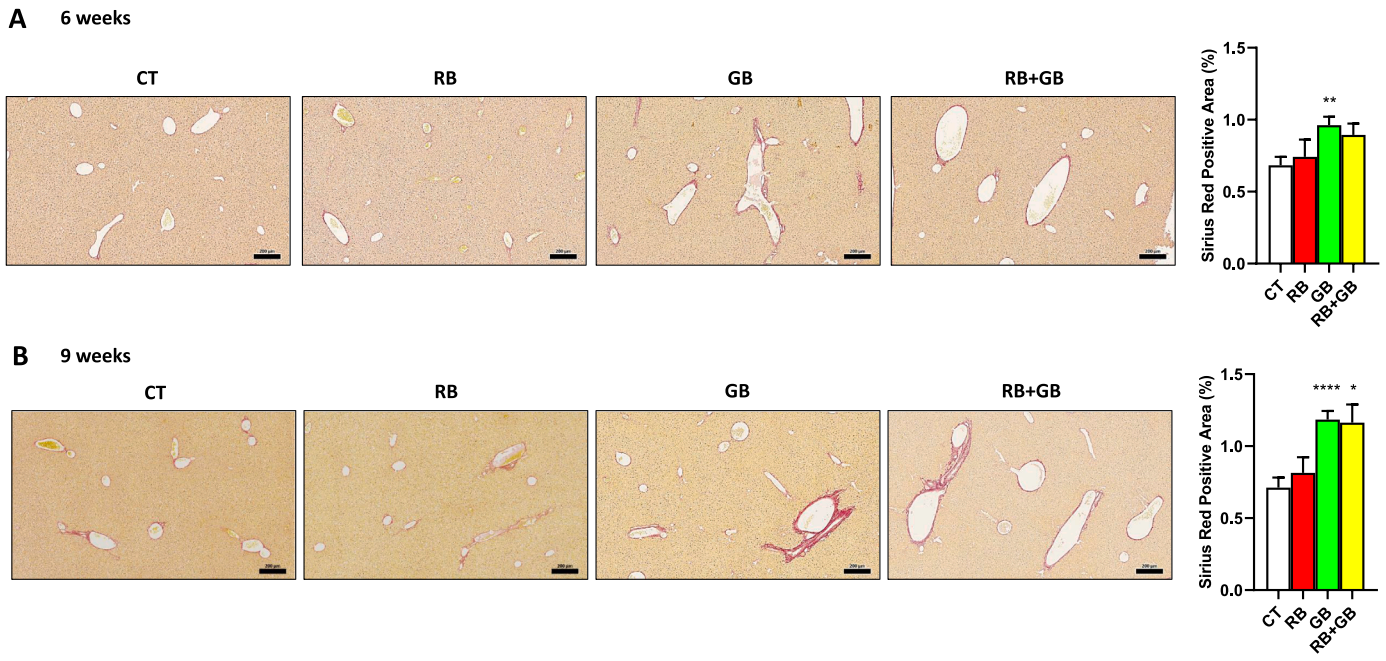

Fig. 6. Effects of polyethylene (PE) exposure on liver HSC activation. Mice were exposed to food spiked with 100 μg/g of PE microbeads (red beads (RB), green beads (GB), or RB+GB; n = 10/group) or control food (CT; n = 10) for 6 and 9 weeks. Representative images of liver sections stained with sirius red and sirius red-positive area quantification. A: 6 weeks exposure. B: 9 weeks exposure. * $p < 0.05$, * * $p < 0.01$, and * ** * $p < 0.001$ compared to the control group as determined by the Mann-Whitney U test.

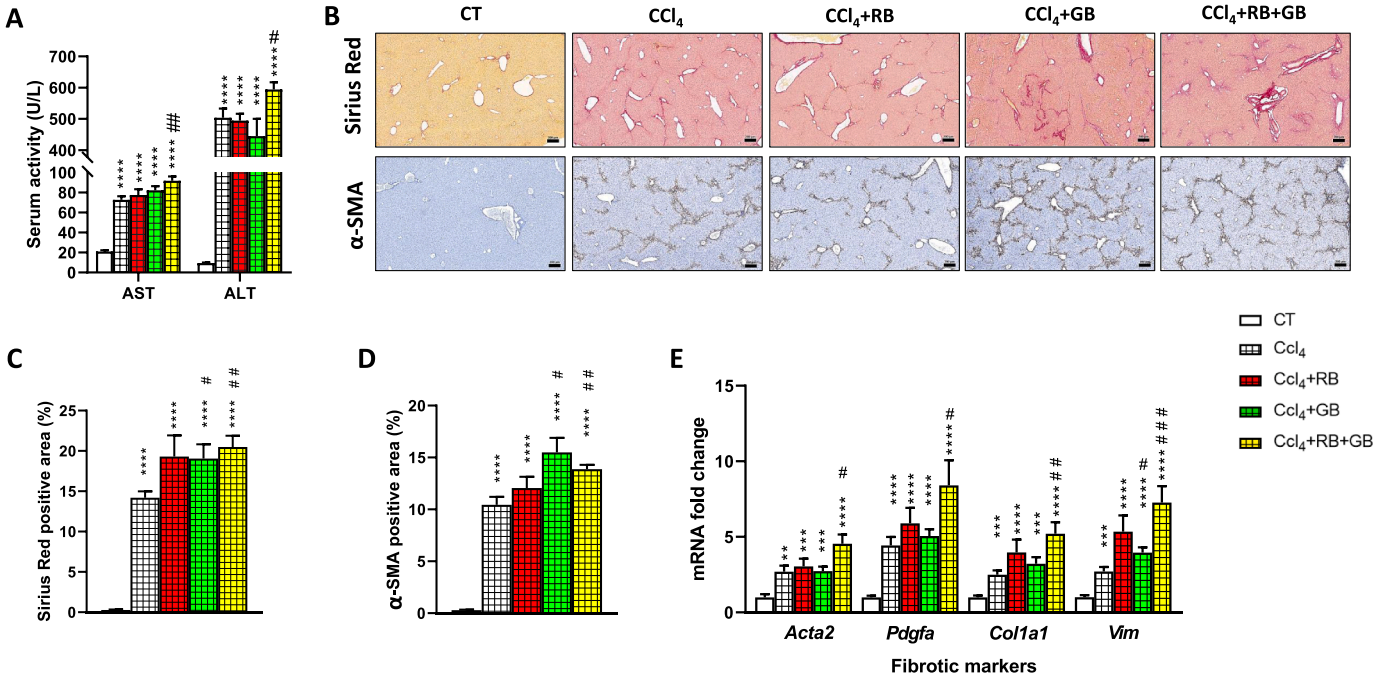

Fig. 7. Effects of polyethylene (PE) exposure on susceptibility to liver fibrosis. Mice were exposed to food spiked with 100 μg/g of PE microbeads (red beads (RB), green beads (GB), or RB+GB) or control food for 8 weeks (n = 8/group). Mice were administered carbon tetrachloride (CCl_4; 0.2 ml/kg bw) to induce liver fibrosis or olive oil as a control (CT) by *i.p.* injection once a week for 8 weeks. (A) Serum alanine transaminase (ALT) and aspartate aminotransferase (AST) activity levels. (B) Representative images of liver sections stained with sirius red (upper panel) and α-SMA (lower panel). (C) Sirius red-positive area quantification. (D) α-SMA-positive area quantification. (E) mRNA quantification of liver fibrotic markers. * $p < 0.05$, * * $p < 0.01$, * ** $p < 0.005$, and * ** * $p < 0.001$ compared to the control group; # $p < 0.05$, ## $p < 0.01$, and ### $p < 0.005$ compared to the CCl_4 group, as determined by the Mann-Whitney U test.

exposed to uncontaminated food. Consistent with these results, biomarkers of hepatic fibrosis, including *Acta2, Pdgfa*, collagen alpha-1(I) chain (*Col1a1*), and vimentin (*Vim*), were significantly upregulated in the 4 groups of mice repeatedly exposed to CCl_4 (Fig. 7E). Exposure to GB enhanced the upregulation of *Vim* in liver as compared to control food. Exposure to RB+GB significantly enhanced the expression of *Acta2, Pdgfa*, *Col1a1*, and *Vim* transcripts in liver. As a whole, these results show that dietary PE exposure exacerbated CCl_4-induced liver

fibrosis.

4. Discussion

PE is the second-most commonly used commercial polymer. It is used in various industries, including agricultural mulches, composite materials, and packaging (El-Sherif et al., 2022). PE is the predominant polymer in personal care products as well as marine samples (Akanyange et al., 2022), and among the most frequently detected MP polymers in food, water, and beverages (Vitali et al., 2022). Increasing evidence indicates that dietary exposure to PE MPs alters morphology, mucin release, and immune and inflammatory responses in the gut (Djouina et al., 2022a; Li et al., 2020; Sun et al., 2021). Moreover, it disturbs intestinal microbiota composition and metabolism (Djouina et al., 2022a; Li et al., 2020; Sun et al., 2021). However, less is known about the effects of PE on liver. In this study, we evaluated the hepatotoxicity of PE MPs after 6- and 9-week exposures. Two different average sizes of PE microbeads were used, 36 μm (RB) and 116 μm (GB), either individually or in combination. Since hallmarks of hepatotoxicity have been described following mouse exposure to MPs composed of other polymers, we investigated whether PE RB and GB can cause similar adverse hepatic effects.

The PE MPs studied are of 36 and 116 μm average diameter size. The 2 types of MPs were chosen in order to reproduce what has been detected in human feces (N. Zhang et al., 2021b). There was about a 3-fold difference in diameter between the 2 types of MPs, in order to raise the issue of size-dependency of MP hepatoxic effects. No parameter showed opposite variation between 36 and 116 μm MPs. The variations observed in our study were either common or specific to the 2 types of MPs. For example, after 9-week exposure, the increase of Cd36, Acaca, and Mttp was common between 36 and 116 μm MPs, the downregulation of Fabp1 and Acox1 was specific to 36 μm MPs, and the upregulation of Slc27a2, Cpt1a, Pparg, Gpam was specific to 116 μm MPs. At first glance, the dissimilarity between 36 and 116 μm MPs cannot be explained by a difference in the cell internalization pathway, since the 2 types of MPs are too large to be internalized by liver or immune cells (Beijer et al., 2022; Stock et al., 2021). However, our data do not allow to determine whether the administered MPs were degraded by digestion, which would have resulted in bringing liver cells into contact with MPs of internalizable size. Literature data on the fate of ingested PM are contradictory. *In vitro*, two studies argue against PE degradation through digestion. Stock et al. showed that artificial in vitro digestion of 4 μm PS particles modified their surface and increased their size. Such changes did not occur for 67 μm PP, 136 μm PVC, 60 μm PET, and notably 90 μm PE MPs (Stock et al., 2020). Fournier et al. exposed 1–10 μm PE MPs to the mucosal artificial colon M-ARCOL, a one-stage fermentation system, which simulates the mean physico-chemical and microbial parameters of the human colon, including not only the luminal but also mucosal microbiota through an external mucin-alginate beads compartment. They did not observe major changes in the polymeric surface composition of PE MPs (Fournier et al., 2023). By contrast, Tamargo et al. subjected PET MPs to digestion simulation in a standardized in vitro static model and to gut-microbial dynamic fermentation using the simgi® model. They observed structural degradation of the PET MPs during the gastrointestinal digestion (Tamargo et al., 2022). *In vivo*, the studies have reported inconsistent findings on liver accumulation of smaller MPs as compared with the one used in the current work. In a first study, Deng et al. showed that both 5 and 20 μm PS MP accumulated in liver after 28-day oral exposure (Deng et al., 2017). By contrast, after 21 weeks of exposure to the PS MPs (40–100 μm), no notable accumulation of MPs was observed in the gut or liver, although mice exhibited gut microbiota dysbiosis, tissue inflammation, and plasma lipid metabolism disorder (Deng et al., 2022). Lee et al. exposed mice to 10–50 μm PE MPs for 28 days. No particles were detected in the liver, spleen, kidney, or heart, while MPs were found in lung, stomach, duodenum, ileum, and serum (Lee et al., 2022). Lastly, the findings of Zaheer et al. suggested that, in mice fed with 10–20 μm PE MPs for 1 week, PE MPs digested in the stomach were deposited into the gut, and the smaller-sized PE fragments transitioned and accumulated in the brain (Zaheer et al., 2022). In view of these studies, it seems unlikely that PE MPs reached the liver in our experimental conditions. Therefore, the effects are more likely to be mediated indirectly, in particular through the effects of MPs on dysbiosis and intestinal immunity, themselves differently impacted depending on the size of the ingested MPs (Djouina et al., 2022b).

In the current work, two times of exposure, 6 or 9 weeks, were evaluated. The effects of MP exposure are known to be time-dependent (Dolar et al., 2022; Shi et al., 2022; Xue et al., 2021), and our aim was to identify common effects between both exposure time and therefore to highlight and rather focus on long lasting effects. After 6-week exposure, 36 μm PE MP exposure decreased liver lipid peroxidation, whereas it increased it after 9-week exposure. The time-dependent effects of MP on oxidative stress has been previously reported in earthworm and bivalves (Lackmann et al., 2022; Z. Li et al., 2022; L. Li et al., 2022). In liver of mice exposed for 1 week to 1 μm PS MP, the major metabolic response was related to oxidative stress, which was no longer the case after 2-week exposure (Shi et al., 2022). Our findings further confirm that MPs exert a time-dependent effect on liver oxidative and antioxidative balance.

Results showed that PE ingestion enhanced the transcriptional expression of several genes involved in fatty acid metabolism. Most notably, *Acaca* was elevated in mice exposed to both PE microbeads either individually or in combination and at both endpoints. This gene is responsible for catalyzing the rate-limiting step of *de novo* lipogenesis and regulates fatty acid β-oxidation in hepatocyte (Bates et al., 2020). In addition to its role of lipid accumulation in hepatocytes, ACACA promotes HSC activation and thus fibrosis, which is in accordance with our results regarding HSC and fibrosis. PE ingestion also led to increased cholesterol and triglyceride levels.

Liver lipid metabolism has previously been studied in response to PS MP ingestion. In contrast to PE, ingestion of PS MPs in drinking water (100 and 1000 μg/l for 5 weeks) decreased *Cd36* and *Pparg* mRNA expression, leading to decreased triglyceride and total cholesterol liver accumulation (Lu et al., 2018). Aged PS MPs were shown to decrease relative mRNA expression of liver *Srebp1c*, *Fasn*, and *Scd1*, favoring a decrease of lipid accumulation in liver similarly to PS MPs (Yang et al., 2022). It is important to note that the latter study observed these outcomes only in female mice, indicating that the effects of PS MPs in liver lipid metabolism are sex-specific. Moreover, maternal exposure to PS MPs in drinking water during gestation decreased total cholesterol hepatic levels in both male and female offspring, which was associated with downregulation of numerous genes involved in fatty acid uptake, β-oxidation, and synthesis (Luo et al., 2019). Similarly, PVC ingestion (0.5 mg/day for 60 days) induced decreased hepatic triglyceride levels (Chen et al., 2022). Therefore, the effects of PE appear to be opposite compared to PS and PVC, since our data supports hepatic lipid accumulation by PE. The effect on lipid digestion is also different between types of polymers. Using an in vitro gastrointestinal digestion model, PS, PET, PE, PVC, and polylactic-co-glycolic acid reduced lipid digestion, and PS had the strongest inhibition (Tan et al., 2020). In this study, two mechanisms were identified for PS effects on lipid digestion: (1) PS MPs decreased the bioavailability of lipid droplets via forming large lipid-MPs heteroaggregates due to the high MP hydrophobicity; and (2) PS MPs adsorbed lipase, and reduced its activity by changing the secondary structure and disturbing the essential open conformation. Further studies are needed to better understand how polymers interact with lipids.

Ingestion of PE significantly induced the expression of xenobiotic metabolizing enzyme expression. For example, *Cyp2a4* expression was upregulated by both RB and GB, either individually or in combination, at 6- and 9-week exposures. CYP2A4 expression is strongly female-biased (female/male ratio of ~1000) and catalyzes testosterone

hydroxylation (Nail et al., 2021). CYP2A4 has a broad substrate specificity, including steroid hormones, lipids, and other xenobiotics such as cadmium (Wang et al., 2022). Other liver defense mechanisms include genes encoding nitric oxide synthase 2 and catalase as well as *Nfe2l2*, *Nqo1*, and *Hmox1*. PE ingestion modulates genes that regulate oxidative stress, which is consistent with other studies that show liver oxidative damage following ingestion of PS MPs (Li et al., 2021; Mu et al., 2022), PS nanospheres (Yasin et al., 2022), and PVC MPs (Chen et al., 2022).

Our results demonstrate that PE can induce low-grade inflammation in liver as shown by the increased presence of hepatic inflammatory foci and upregulation of inflammatory cytokines. Similarly, exposure to PS MPs (500 and 1000 mg/l) caused IL-1β secretion in liver (Mu et al., 2022), and exposure to PS MPs (0.5 mg/mouse) increased the infiltration of natural killer cells and macrophages to non-parenchymal liver cells and dysregulated the expression of several cytokines (Zhao et al., 2021). Although pro-oxidative and pro-inflammatory effects are predominant in hepatic response to PE MP exposure, anti-inflammatory response was also observed. For example, 116 μm PE MP exposure led to Il1b downregulation after 6- and 9-week exposure. These findings are in accordance with results obtained with human cell lines, showing that PE MP exposure induced pro-inflammatory cytokine response in keratinocytes, whereas opposite effect was observed in THP-1 and U937 immune cells (Gautam et al., 2022). The MP induced cell-specific immune modulation remains to be elucidated.

PE MP ingestion led to hyperproliferation of the liver which can have potential consequences for the promotion of hepatocarcinogenesis. Based on hepatic cell markers and collagen deposition staining, our data suggests that HSCs could be the target of hyperproliferation which prompted an investigation into the effects of PE ingestion on liver fibrosis susceptibility. PE exposure was found to increase the severity of CCl_4-induced hepatic fibrosis, which is based on data showing a significant elevation of collagen and α-SMA deposition in liver as well as enhanced expression of several fibrotic markers.

Shen et al. demonstrated that PS MPs administrated at either 0.1 or 1 mg/l in drinking water for 60 days was sufficient to induce development of severe liver fibrosis in mice. In contrast, sub-chronic PE dietary contamination induced weak liver fibrosis under healthy conditions, and worsened fibrogenesis under profibrotic conditions. It is not possible at this time to determine whether these dissimilarities on fibrosis outcomes were due to differences in experimental design or chemical differences in the polymers. Other studies have also shown that polymer MPs can worsen preconditions. For example, exposure to PS was shown to exacerbate cyclophosphamide and acetaminophen-induced liver injury (Liu et al., 2022; Wen et al., 2022). Moreover, PS NPs potentiated the development of hepatic fibrosis in mice fed a high-fat diet (Z. Li et al., 2022; L. Li et al., 2022). These results raise concerns that MP exposure could aggravate pre-existing liver pathologies in susceptible individuals.

More research is necessary to determine the human relevance of these results. Recent studies, however, have started to explore the effects of PS in human pluripotent stem cell-derived liver organoids (Cheng et al., 2022a, 2022b). Several hallmarks of hepatoxicity, such as increased inflammation and compromised antioxidative balance, observed in vivo have been confirmed in human liver organoids. Fatty acid β-oxidation inhibition leading to steatosis was also consistently observed in mouse studies and in human liver organoids. In addition, an increase in the fibrotic marker *Col1a1* was also detected in liver organoids (Cheng et al., 2022a).

5. Conclusion

In summary, the present study demonstrated that PE MP food contamination alters defense mechanisms and promotes lipid accumulation, low-grade inflammation, and cell proliferation in mouse liver. Dietary PE exposure worsened fibrogenesis in a model of CCl_4-induced liver fibrosis. This study shows that PE exposure, similarly to PS, can lead to adverse effects in the liver. Overall, these findings confirm that ubiquitous contamination by MPs has the potential to contribute to the aggravation of chronic liver pathologies.

Funding sources

This study was supported by the French Region Hauts-de-France.

CRediT authorship contribution statement

Madjid Djouina: Methodology, Formal analysis, Investigation, Writing – original draft. **Christophe Waxin:** Formal analysis, Investigation. **Laurent Dubuquoy:** Writing – review & editing, Funding acquisition. **David Launay:** Funding acquisition. **Cécile Vignal:** Writing – review & editing, Funding acquisition. **Mathilde Body-Malapel:** Conceptualization, Methodology, Validation, Formal analysis, Writing – original draft, Supervision, Funding acquisition.

Declaration of Competing Interest

The authors declare that they have no known competing financial interests or personal relationships that could have appeared to influence the work reported in this paper.

Data availability

Data will be made available on request.

Acknowledgments

We thank Guillaume Duflos from ANSES – Laboratoire de Sécurité des Aliments for providing the PE microbeads. We also thank Meryem Tardivel and Marie-Hélène Gevaert from Platforms Lilloises in Biology and Health (PLBS) - UMS 2014 - US 41 for technical assistance on analysis and section cutting, respectively, as well as Thomas Hubert and the staff of the animal facility of Lille, for animal care. We thank François Maggiotto for technical assistance. Editorial assistance, in the form of language editing and correction, was provided by XpertScientific Editing and Consulting Services.

Appendix A. Supporting information

Supplementary data associated with this article can be found in the online version at doi:10.1016/j.ecoenv.2023.115417.

References

Akanyange, S.N., Zhang, Y., Zhao, X., Adom-Asamoah, G., Ature, A.-R.A., Anning, C., Tianpeng, C., Zhao, H., Lyu, X., Crittenden, J.C., 2022. A holistic assessment of microplastic ubiquitousness: Pathway for source identification in the environment. Sustain. Prod. Consum 33, 113–145. https://doi.org/10.1016/j.spc.2022.06.020.

Bai, C.-L., Liu, L.-Y., Hu, Y.-B., Zeng, E.Y., Guo, Y., 2022. Microplastics: A review of analytical methods, occurrence and characteristics in food, and potential toxicities to biota. Sci. Total Environ. 806, 150263 https://doi.org/10.1016/j.scitotenv.2021.150263.

Bankhead, P., Loughrey, M.B., Fernández, J.A., Dombrowski, Y., McArt, D.G., Dunne, P. D., McQuaid, S., Gray, R.T., Murray, L.J., Coleman, H.G., James, J.A., Salto-Tellez, M., Hamilton, P.W., 2017. QuPath: Open source software for digital pathology image analysis. Sci. Rep. 7, 16878. https://doi.org/10.1038/s41598-017-17204-5.

Bates, J., Vijayakumar, A., Ghoshal, S., Marchand, B., Yi, S., Kornyeyev, D., Zagorska, A., Hollenback, D., Walker, K., Liu, K., Pendem, S., Newstrom, D., Brockett, R., Mikaelian, I., Kusam, S., Ramirez, R., Lopez, D., Li, L., Fuchs, B.C., Breckenridge, D. G., 2020. Acetyl-CoA carboxylase inhibition disrupts metabolic reprogramming during hepatic stellate cell activation. J. Hepatol. 73, 896–905. https://doi.org/10.1016/j.jhep.2020.04.037.

Beijer, N.R.M., Dehaut, A., Carlier, M.P., Wolter, H., Versteegen, R.M., Pennings, J.L.A., de la Fonteyne, L., Niemann, H., Janssen, H.M., Timmermans, B.G., Mennes, W., Cassee, F.R., Mengelers, M.J.B., Amaral-Zettler, L.A., Duflos, G., Staal, Y.C.M., 2022. Relationship Between Particle Properties and Immunotoxicological Effects of Environmentally-Sourced Microplastics. Front. Water 4.

Braun, T., Ehrlich, L., Henrich, W., Koeppel, S., Lomako, I., Schwabl, P., Liebmann, B., 2021. Detection of microplastic in human placenta and meconium in a clinical setting. Pharmaceutics 13, 921. https://doi.org/10.3390/pharmaceutics13070921.

Campana, L., Esser, H., Huch, M., Forbes, S., 2021. Liver regeneration and inflammation: from fundamental science to clinical applications. Nat. Rev. Mol. Cell Biol. 22, 608–624.

Chen, X., Zhuang, J., Chen, Q., Xu, L., Yue, X., Qiao, D., 2022. Chronic exposure to polyvinyl chloride microplastics induces liver injury and gut microbiota dysbiosis based on the integration of liver transcriptome profiles and full-length 16S rRNA sequencing data. Sci. Total Environ. 839, 155984 https://doi.org/10.1016/j.scitotenv.2022.155984.

Cheng, W., Li, X., Zhou, Y., Yu, H., Xie, Y., Guo, H., Wang, H., Li, Y., Feng, Y., Wang, Y., 2022a. Polystyrene microplastics induce hepatotoxicity and disrupt lipid metabolism in the liver organoids. Sci. Total Environ. 806, 150328 https://doi.org/10.1016/j.scitotenv.2021.150328.

Cheng, W., Zhou, Y., Xie, Y., Li, Y., Zhou, R., Wang, H., Feng, Y., Wang, Y., 2022b. Combined effect of polystyrene microplastics and bisphenol A on the human embryonic stem cells-derived liver organoids: The hepatotoxicity and lipid accumulation. Sci. Total Environ., 158585 https://doi.org/10.1016/j.scitotenv.2022.158585.

da Costa Araújo, A.P., Gomes, A.R., Malafaia, G., 2020. Hepatotoxicity of pristine polyethylene microplastics in neotropical Physalaemus cuvieri tadpoles (Fitzinger, 1826. J. Hazard. Mater. 386, 121992.

Deng, Y., Zhang, Y., Lemos, B., Ren, H., 2017. Tissue accumulation of microplastics in mice and biomarker responses suggest widespread health risks of exposure. Sci. Rep. 7, 46687. https://doi.org/10.1038/srep46687.

Deng, Y., Chen, H., Huang, Y., Zhang, Y., Ren, H., Fang, M., Wang, Q., Chen, W., Hale, R. C., Galloway, T.S., Chen, D., 2022. Long-Term Exposure to Environmentally Relevant Doses of Large Polystyrene Microplastics Disturbs Lipid Homeostasis via Bowel Function Interference. Environ. Sci. Technol. 56, 15805–15817. https://doi.org/10.1021/acs.est.1c07933.

Djouina, M., Vignal, C., Dehaut, A., Caboche, S., Hirt, N., Waxin, C., Himber, C., Beury, D., Hot, D., Dubuquoy, L., Launay, D., Duflos, G., Body-Malapel, M., 2022a. Oral exposure to polyethylene microplastics alters gut morphology, immune response, and microbiota composition in mice. Environ. Res. 212, 113230 https://doi.org/10.1016/j.envres.2022.113230.

Djouina, M., Vignal, C., Dehaut, A., Caboche, S., Hirt, N., Waxin, C., Himber, C., Beury, D., Hot, D., Dubuquoy, L., Launay, D., Duflos, G., Body-Malapel, M., 2022b. Oral exposure to polyethylene microplastics alters gut morphology, immune response, and microbiota composition in mice. Environ. Res. 212, 113230 https://doi.org/10.1016/j.envres.2022.113230.

Dolar, A., Drobne, D., Dolenec, M., Marinšek, M., Jemec Kokalj, A., 2022. Time-dependent immune response in Porcellio scaber following exposure to microplastics and natural particles. Sci. Total Environ. 818, 151816 https://doi.org/10.1016/j.scitotenv.2021.151816.

Dong, R., Zhou, C., Wang, S., Yan, Y., Jiang, Q., 2022. Probiotics ameliorate polyethylene microplastics-induced liver injury by inhibition of oxidative stress in Nile tilapia (Oreochromis niloticus). Fish. Shellfish Immunol. 130, 261–272.

Dubuquoy, L., Louvet, A., Lassailly, G., Truant, S., Boleslawski, E., Artru, F., Maggiotto, F., Gantier, E., Buob, D., Leteurtre, E., Cannesson, A., Dharancy, S., Moreno, C., Pruvot, F.-R., Bataller, R., Mathurin, P., 2015. Progenitor cell expansion and impaired hepatocyte regeneration in explanted livers from alcoholic hepatitis. Gut 64, 1949–1960. https://doi.org/10.1136/gutjnl-2014-308410.

El-Sherif, D.M., Eloffy, M.G., Elmesery, A., Abouzid, M., Gad, M., El-Seedi, H.R., Brinkmann, M., Wang, K., Al Naggar, Y., 2022. Environmental risk, toxicity, and biodegradation of polyethylene: a review. Environ. Sci. Pollut. Res. 29, 81166–81182. https://doi.org/10.1007/s11356-022-23382-1.

Ferronato, N., Torretta, V., 2019. Waste Mismanagement in Developing Countries: A Review of Global Issues. Int. J. Environ. Res. Public. Health 16, 1060. https://doi.org/10.3390/ijerph16061060.

Fournier, E., Leveque, M., Ruiz, P., Ratel, J., Durif, C., Chalancon, S., Amiard, F., Edely, M., Bezirard, V., Gaultier, E., Lamas, B., Houdeau, E., Lagarde, F., Engel, E., Etienne-Mesmin, L., Blanquet-Diot, S., Mercier-Bonin, M., 2023. Microplastics: What happens in the human digestive tract? First evidences in adults using in vitro gut models. J. Hazard. Mater. 442, 130010 https://doi.org/10.1016/j.jhazmat.2022.130010.

Gasperi, J., Wright, S.L., Dris, R., Collard, F., Mandin, C., Guerrouache, M., Langlois, V., Kelly, F.J., Tassin, B., 2018, Microplastics in air: Are we breathing it in? Curr. Opin. Environ. Sci. Health, Micro and Nanoplastics Edited by Dr. Teresa A.P. Rocha-Santos 1, 1–5. https://doi.org/10.1016/j.coesh.2017.10.002.

Gautam, R., Jo, J., Acharya, M., Maharjan, A., Lee, D., K.c, P.B., Kim, C., Kim, K., Kim, H., Heo, Y., 2022. Evaluation of potential toxicity of polyethylene microplastics on human derived cell lines. Sci. Total Environ. 838, 156089 https://doi.org/10.1016/j.scitotenv.2022.156089.

Hirt, N., Body-Malapel, M., 2020. Immunotoxicity and intestinal effects of nano-and microplastics: a review of the literature. Part. Fibre Toxicol. 17, 1–22. https://doi.org/10.1186/s12989-020-00387-7.

Horvatits, T., Tamminga, M., Liu, B., Sebode, M., Carambia, A., Fischer, L., Püschel, K., Huber, S., Fischer, E.K., 2022. Microplastics detected in cirrhotic liver tissue. eBioMedicine 82, 104147. https://doi.org/10.1016/j.ebiom.2022.104147.

Hu, J., Zuo, J., Li, J., Zhang, Y., Ai, X., Zhang, J., Gong, D., Sun, D., 2022. Effects of secondary polyethylene microplastic exposure on crucian (Carassius carassius) growth, liver damage, and gut microbiome composition. Sci. Total Environ. 802, 149736 https://doi.org/10.1016/j.scitotenv.2021.149736.

Huang, D., Zhang, Y., Long, J., Yang, X., Bao, L., Yang, Z., Wu, B., Si, R., Zhao, W., Peng, C., Wang, A., Yan, D., 2022. Polystyrene microplastic exposure induces insulin resistance in mice via dysbacteriosis and pro-inflammation. Sci. Total Environ. 838, 155937 https://doi.org/10.1016/j.scitotenv.2022.155937.

Ibrahim, Y.S., Anuar, S.T., Azmi, A.A., Khalik, W.M.A.W.M., Lehata, S., Hamzah, S.R., Ismail, D., Ma, Z.F., Dzulkarnaen, A., Zakaria, Z., Mustaffa, N., Sharif, S.E.T., Lee, Y. Y., 2021. Detection of microplastics in human colectomy specimens. JGH Open 5, 116–121. https://doi.org/10.1002/jgh3.12457.

Im, C., Kim, H., Zaheer, J., Kim, J.Y., Lee, Y.-J., Kang, C.M., Kim, J.S., 2022. PET Tracing of Biodistribution for Orally Administered 64Cu-Labeled Polystyrene in Mice. J. Nucl. Med. 63, 461–467. https://doi.org/10.2967/jnumed.120.256982.

Lackmann, C., Velki, M., Šimić, A., Müller, A., Braun, U., Ečimović, S., Hollert, H., 2022. Two types of microplastics (polystyrene-HBCD and car tire abrasion) affect oxidative stress-related biomarkers in earthworm Eisenia andrei in a time-dependent manner. Environ. Int. 163, 107190 https://doi.org/10.1016/j.envint.2022.107190.

Lee, Sijoon, Kang, K.-K., Sung, S.-E., Choi, J.-H., Sung, M., Seong, K.-Y., Lee, Sunjong, Yang, S.Y., Seo, M.-S., Kim, K., 2022. Toxicity study and quantitative evaluation of polyethylene microplastics in ICR mice. Polymers 14, 402. https://doi.org/10.3390/polym14030402.

Leslie, H.A., van Velzen, M.J.M., Brandsma, S.H., Vethaak, A.D., Garcia-Vallejo, J.J., Lamoree, M.H., 2022. Discovery and quantification of plastic particle pollution in human blood. Environ. Int. 163, 107199 https://doi.org/10.1016/j.envint.2022.107199.

Li, B., Ding, Y., Cheng, X., Sheng, D., Xu, Z., Rong, Q., Wu, Y., Zhao, H., Ji, X., Zhang, Y., 2020. Polyethylene microplastics affect the distribution of gut microbiota and inflammation development in mice. Chemosphere 244, 125492. https://doi.org/10.1016/j.chemosphere.2019.125492.

Li, L., Xu, M., He, C., Wang, H., Hu, Q., 2022. Polystyrene nanoplastics potentiate the development of hepatic fibrosis in high fat diet fed mice. Environ. Toxicol. 37, 362–372. https://doi.org/10.1002/tox.23404.

Li, S., Shi, M., Wang, Y., Xiao, Y., Cai, D., Xiao, F., 2021. Keap1-Nrf2 pathway up-regulation via hydrogen sulfide mitigates polystyrene microplastics induced-hepatotoxic effects. J. Hazard. Mater. 402, 123933 https://doi.org/10.1016/j.jhazmat.2020.123933.

Li, Z., Chang, X., Hu, M., Fang, J.K.-H., Sokolova, I.M., Huang, W., Xu, E.G., Wang, Y., 2022. Is microplastic an oxidative stressor? Evidence from a meta-analysis on bivalves. J. Hazard. Mater. 423, 127211 https://doi.org/10.1016/j.jhazmat.2021.127211.

Lim, X., 2021. Microplastics are everywhere - but are they harmful? Nature 593, 22–25. https://doi.org/10.1038/d41586-021-01143-3.

Liu, J., Zhang, L., Xu, F., Meng, S., Li, H., Song, Y., 2022. Polystyrene Microplastics Postpone APAP-Induced Liver Injury through Impeding Macrophage Polarization. Toxics 10, 792. https://doi.org/10.3390/toxics10120792.

Lu, L., Wan, Z., Luo, T., Fu, Z., Jin, Y., 2018. Polystyrene microplastics induce gut microbiota dysbiosis and hepatic lipid metabolism disorder in mice. Sci. Total Environ. 631–632, 449–458. https://doi.org/10.1016/j.scitotenv.2018.03.051.

Lu, X., Zhang, J.-X., Zhang, L., Wu, D., Tian, J., Yu, L.-J., He, L., Zhong, S., Du, H., Deng, D.-F., 2022. Negative impacts of chronic dietary exposure to polyethylene microplastics on growth, gut microbiota, liver metabolism and gene expressions in genetically improved farmed tilapia (Oreochromis niloticus). Sci. Total Environ., 156571

Luo, T., Zhang, Y., Wang, C., Wang, X., Zhou, J., Shen, M., Zhao, Y., Fu, Z., Jin, Y., 2019. Maternal exposure to different sizes of polystyrene microplastics during gestation causes metabolic disorders in their offspring. Environ. Pollut. Barking Essex 1987 (255), 113122. https://doi.org/10.1016/j.envpol.2019.113122.

Luo, T., Wang, D., Zhao, Y., Li, X., Yang, G., Jin, Y., 2022. Polystyrene microplastics exacerbate experimental colitis in mice tightly associated with the occurrence of hepatic inflammation. Sci. Total Environ. 844, 156884 https://doi.org/10.1016/j.scitotenv.2022.156884.

Luqman, A., Nugrahapraja, H., Wahyuono, R.A., Islami, I., Haekal, M.H., Fardiansyah, Y., Putri, B.Q., Amalludin, F.I., Rofiqa, E.A., Götz, F., Wibowo, A.T., 2021. Microplastic Contamination in Human Stools, Foods, and Drinking Water Associated with Indonesian Coastal Population. Environments 8, 138. https://doi.org/10.3390/environments8120138.

Mak, C.W., Yeung, K.C.-F., Chan, K.M., 2019. Acute toxic effects of polyethylene microplastic on adult zebrafish. Ecotoxicol. Environ. Saf. 182, 109442.

Mohamed Nor, N.H., Kooi, M., Diepens, N.J., Koelmans, A.A., 2021. Lifetime Accumulation of Microplastic in Children and Adults. Environ. Sci. Technol. 55, 5084–5096. https://doi.org/10.1021/acs.est.0c07384.

Mortensen, N.P., Fennell, T.R., Johnson, L.M., 2021. Unintended human ingestion of nanoplastics and small microplastics through drinking water, beverages, and food sources. NanoImpact 21, 100302. https://doi.org/10.1016/j.impact.2021.100302.

Mu, Y., Sun, J., Li, Z., Zhang, W., Liu, Z., Li, C., Peng, C., Cui, G., Shao, H., Du, Z., 2022. Activation of pyroptosis and ferroptosis is involved in the hepatotoxicity induced by polystyrene microplastics in mice. Chemosphere 291, 132944. https://doi.org/10.1016/j.chemosphere.2021.132944.

Nail, A.N., Spear, B.T., Peterson, M.L., 2021. Highly homologous mouse Cyp2a4 and Cyp2a5 genes are differentially expressed in the liver and both express long non-coding antisense RNAs. Gene 767, 145162. https://doi.org/10.1016/j.gene.2020.145162.

Oliveira, F.M.S., da Paixão Matias, P.H., Kraemer, L., Gazzinelli-Guimarães, A.C., Santos, F.V., Amorim, C.C.O., Nogueira, D.S., Freitas, C.S., Caliari, M.V., Bartholomeu, D.C., 2019. Comorbidity associated to Ascaris suum infection during pulmonary fibrosis exacerbates chronic lung and liver inflammation and dysfunction but not affect the parasite cycle in mice. PLoS Negl. Trop. Dis. 13, e0007896.

Saleh, M.B., Louvet, A., Ntandja-Wandji, L.C., Boleslawski, E., Gnemmi, V., Lassailly, G., Truant, S., Maggiotto, F., Ningarhari, M., Artru, F., 2021. Loss of hepatocyte identity

following aberrant YAP activation: a key mechanism in alcoholic hepatitis. J. Hepatol. 75, 912–923.
Schwabl, P., Köppel, S., Königshofer, P., Bucsics, T., Trauner, M., Reiberger, T., Liebmann, B., 2019. Detection of various microplastics in human stool: a prospective case series. Ann. Intern. Med. https://doi.org/10.7326/M19-0618.
Senathirajah, K., Attwood, S., Bhagwat, G., Carbery, M., Wilson, S., Palanisami, T., 2021. Estimation of the mass of microplastics ingested – A pivotal first step towards human health risk assessment. J. Hazard. Mater. 404, 124004 https://doi.org/10.1016/j.jhazmat.2020.124004.
Shi, C., Han, X., Guo, W., Wu, Q., Yang, X., Wang, Y., Tang, G., Wang, S., Wang, Z., Liu, Y., Li, M., Lv, M., Guo, Y., Li, Z., Li, J., Shi, J., Qu, G., Jiang, G., 2022. Disturbed Gut-Liver axis indicating oral exposure to polystyrene microplastic potentially increases the risk of insulin resistance. Environ. Int. 164, 107273 https://doi.org/10.1016/j.envint.2022.107273.
Song, Y.K., Hong, S.H., Jang, M., Han, G.M., Jung, S.W., Shim, W.J., 2017. Combined Effects of UV Exposure Duration and Mechanical Abrasion on Microplastic Fragmentation by Polymer Type. Environ. Sci. Technol. 51, 4368–4376. https://doi.org/10.1021/acs.est.6b06155.
Stock, V., Fahrenson, C., Thuenemann, A., Dönmez, M.H., Voss, L., Böhmert, L., Braeuning, A., Lampen, A., Sieg, H., 2020. Impact of artificial digestion on the sizes and shapes of microplastic particles. Food Chem. Toxicol. 135, 111010 https://doi.org/10.1016/j.fct.2019.111010.
Stock, V., Laurisch, C., Franke, J., Dönmez, M.H., Voss, L., Böhmert, L., Braeuning, A., Sieg, H., 2021. Uptake and cellular effects of PE, PP, PET and PVC microplastic particles. Toxicol. Vitr. 70, 105021 https://doi.org/10.1016/j.tiv.2020.105021.
Sun, H., Chen, N., Yang, X., Xia, Y., Wu, D., 2021. Effects induced by polyethylene microplastics oral exposure on colon mucin release, inflammation, gut microflora composition and metabolism in mice. Ecotoxicol. Environ. Saf. 220, 112340 https://doi.org/10.1016/j.ecoenv.2021.112340.
Sun, W., Jin, C., Bai, Y., Ma, R., Deng, Y., Gao, Y., Pan, G., Yang, Z., Yan, L., 2022. Blood uptake and urine excretion of nano- and micro-plastics after a single exposure. Sci. Total Environ. 848, 157639 https://doi.org/10.1016/j.scitotenv.2022.157639.
Tamargo, A., Molinero, N., Reinosa, J.J., Alcolea-Rodriguez, V., Portela, R., Bañares, M. A., Fernández, J.F., Moreno-Arribas, M.V., 2022. PET microplastics affect human gut microbiota communities during simulated gastrointestinal digestion, first evidence of plausible polymer biodegradation during human digestion. Sci. Rep. 12, 528. https://doi.org/10.1038/s41598-021-04489-w.
Tan, H., Yue, T., Xu, Y., Zhao, J., Xing, B., 2020. Microplastics reduce lipid digestion in simulated human gastrointestinal system. Environ. Sci. Technol. 54, 12285–12294. https://doi.org/10.1021/acs.est.0c02608.
Vitali, C., Peters, R., Janssen, H.-G., Nielen, M, W.F., 2022. Microplastics and nanoplastics in food, water, and beverages; part I. Occurrence. TrAC Trends Anal. Chem., 116670 https://doi.org/10.1016/j.trac.2022.116670.
Wang, H., Zhang, L., Xia, Z., Cui, J.Y., 2022. Effect of chronic cadmium exposure on brain and liver transporters and drug-metabolizing enzymes in male and female mice genetically predisposed to Alzheimer's Disease. Drug Metab. Dispos. 50, 1414–1428. https://doi.org/10.1124/dmd.121.000453.
Wang, S., Wu, H., Shi, X., Wang, Y., Xu, S., 2023a. Polystyrene microplastics with different sizes induce the apoptosis and necroptosis in liver through the PTEN/PI3K/AKT/autophagy axis. Sci. Total Environ. 899, 165461 https://doi.org/10.1016/j.scitotenv.2023.165461.
Wang, X., Weng, Y., Geng, S., Wang, C., Jin, C., Shi, L., Jin, Y., 2023b. Maternal procymidone exposure has lasting effects on murine gut-liver axis and glucolipid metabolism in offspring. Food Chem. Toxicol. 174, 113657 https://doi.org/10.1016/j.fct.2023.113657.
Wen, S., Zhao, Y., Liu, S., Chen, Y., Yuan, H., Xu, H., 2022. Polystyrene microplastics exacerbated liver injury from cyclophosphamide in mice: Insight into gut microbiota. Sci. Total Environ. 840, 156668 https://doi.org/10.1016/j.scitotenv.2022.156668.
Wibowo, A.T., Nugrahapraja, H., Wahyuono, R.A., Islami, I., Haekal, M.H., Fardiansyah, Y., Sugiyo, P.W.W., Putro, Y.K., Fauzia, F.N., Santoso, H., Götz, F., Tangahu, B.V., Luqman, A., 2021. Microplastic Contamination in the Human Gastrointestinal Tract and Daily Consumables Associated with an Indonesian Farming Community. Sustainability 13, 12840. https://doi.org/10.3390/su132212840.
Xue, Y.-H., Feng, L.-S., Xu, Z.-Y., Zhao, F.-Y., Wen, X.-L., Jin, T., Sun, Z.-X., 2021. The time-dependent variations of zebrafish intestine and gill after polyethylene microplastics exposure. Ecotoxicology 30, 1997–2010. https://doi.org/10.1007/s10646-021-02469-4.
Yang, W., He, H., Wang, T., Su, N., Zhang, F., Jiang, K., Zhu, J., Zhang, C., Niu, K., Wang, L., Yuan, X., Liu, N., Li, L., Wei, W., Hu, J., 2021. Single-cell transcriptomic analysis reveals a hepatic stellate cell-activation roadmap and myofibroblast origin during liver fibrosis in mice. Hepatol. Baltim Md 74, 2774–2790. https://doi.org/10.1002/hep.31987.
Yang, X., Jiang, J., Wang, Q., Duan, J., Chen, N., Wu, D., Xia, Y., 2022. Gender difference in hepatic AMPK pathway activated lipid metabolism induced by aged polystyrene microplastics exposure. Ecotoxicol. Environ. Saf. 245, 114105 https://doi.org/10.1016/j.ecoenv.2022.114105.
Yasin, N.A.E., El-Naggar, M.E., Ahmed, Z.S.O., Galal, M.K., Rashad, M.M., Youssef, A.M., Elleithy, E.M.M., 2022. Exposure to Polystyrene nanoparticles induces liver damage in rat via induction of oxidative stress and hepatocyte apoptosis. Environ. Toxicol. Pharmacol. 94, 103911 https://doi.org/10.1016/j.etap.2022.103911.
Zaheer, J., Kim, H., Ko, I.O., Jo, E.-K., Choi, E.-J., Lee, H.-J., Shim, I., Woo, H., Choi, J., Kim, G.-H., Kim, J.S., 2022. Pre/post-natal exposure to microplastic as a potential risk factor for autism spectrum disorder. Environ. Int. 161, 107121 https://doi.org/10.1016/j.envint.2022.107121.
Zhang, J., Wang, L., Trasande, L., Kannan, K., 2021a. Occurrence of polyethylene terephthalate and polycarbonate microplastics in infant and adult feces. Environ. Sci. Technol. Lett. https://doi.org/10.1021/acs.estlett.1c00559.
Zhang, N., Li, Y.B., He, H.R., Zhang, J.F., Ma, G.S., 2021b. You are what you eat: Microplastics in the feces of young men living in Beijing. Sci. Total Environ. 767, 144345 https://doi.org/10.1016/j.scitotenv.2020.144345.
Zhao, L., Shi, W., Hu, F., Song, X., Cheng, Z., Zhou, J., 2021. Prolonged oral ingestion of microplastics induced inflammation in the liver tissues of C57BL/6J mice through polarization of macrophages and increased infiltration of natural killer cells. Ecotoxicol. Environ. Saf. 227, 112882 https://doi.org/10.1016/j.ecoenv.2021.112882.
Zheng, H., Wang, J., Wei, X., Chang, L., Liu, S., 2021. Proinflammatory properties and lipid disturbance of polystyrene microplastics in the livers of mice with acute colitis. Sci. Total Environ. 750, 143085 https://doi.org/10.1016/j.scitotenv.2020.143085.